Remote Sensing of Environment 225 (2019) 416–430

Contents lists available at ScienceDirect

Remote Sensing of Environment

journal homepage: www.elsevier.com/locate/rse

Validation of the Sentinel Simplified Level 2 Product Prototype Processor (SL2P) for mapping cropland biophysical variables using Sentinel-2/MSI and Landsat-8/OLI data

Najib Djamai[a,*], Richard Fernandes[a], Marie Weiss[b], Heather McNairn[c], Kalifa Goïta[d]

[a] Canada Centre for Remote Sensing, Natural Resources Canada, 560 Rochester Street, Ottawa, Ontario K1A 0E4, Canada
[b] Institut National de la Recherche Agronomique, Université d'Avignon et des Pays du Vaucluse (INRA-UAPV), 228 Route de l'Aérodrome, 84914 Avignon, France
[c] Agriculture and Agri-Food Canada, 960 Carling Ave, Ottawa, Ontario K1A 0C6, Canada
[d] CARTEL, Université de Sherbrooke, 2500 boul. de l'Université, Sherbrooke, Québec J1K 2R1, Canada

ARTICLE INFO

Keywords:
Vegetation biophysical variables
Sentinel-2/MSI
Landsat-8/OLI
SL2P
Validation

ABSTRACT

The Simplified Level 2 Product Prototype Processor (SL2P) for estimating Leaf Area index (LAI), fraction of vegetation cover (fCover) and Canopy Water Content (CWC) from Sentinel-2/MSI and Landsat-8/OLI data was validated over an agricultural region. In-situ data collected during the SMAP Validation Experiment 2016 field campaign were used as a reference. SL2P processor performance varied substantially between crop type and biophysical variable. Over all crops, SL2P underestimated in-situ LAI and CWC measurements when using either MSI (slope (bias) of 0.70 (−0.37) for LAI and 0.42 (−0.37 kg/m^2) for CWC) or OLI (slope (bias) of 0.59 (−1.21) for LAI and 0.24 (−0.23 kg/m^2) for CWC) data. The accuracy of SL2P fCover estimates, over all crops, was higher (slope (bias) of 0.99 (1.84%) using MSI and 0.93 (−3.75%) using OLI). The RMSE between biophysical variables estimated using SL2P from MSI (OLI) in comparison to in-situ data was 0.98 (1.63) for LAI, 11.39% (10.95%) for fCover and 0.66 kg/m^2 (0.96 kg/m^2) for CWC. Slightly better results are generally obtained using locally calibrated vegetation indices models, when compared to SL2P estimates using the corresponding sensor data. Uncertainty metrics of vegetation biophysical variables derived from both MSI and OLI, when compared to interpolated in-situ data time series, are found comparable to results obtained for cross-validation suggesting the possibility of using interpolated in-situ data time series for validating decametric resolution remote sensing products sparsely sampled in time.

1. Introduction

There is international consensus as to the requirement for systematic 50 m resolution global mapping of vegetation biophysical variables, including leaf area index (LAI), at intervals of ≤10 days (Table 1; Global Climate Observing System (GCOS), 2016). This requirement is supplemented by the need for the global monitoring of agricultural production and risks to food supply (Group on Earth Observations (GEO), 2018). Such monitoring includes mapping LAI and additional cropland biophysical variables, including the fraction of vegetation cover (fCover) and canopy water content (CWC), at decametric resolution (< 100 m). Table 1 provides product specifications based on both GCOS 2016 implementation plan and the Sentinels for Science (SEN4SCI) expert consultation activity (Malenovsky et al., 2012).

Multispectral bi-directional reflectance measurements are related to vegetation canopy biophysical variables (Pearson and Miller, 1972; Suits, 1972; Ross, 1975; Bunnik, 1978). These relationships have led to algorithms for retrieval of biophysical variables from multispectral satellite imagery first using regressions between reflectance and in-situ measurements (Kanemasu, 1974; Polloc and Kanemasu, 1979; Weigand et al., 1979; Chance, 1981; Kimes et al., 1981; Asrar et al., 1985; Best and Harlan, 1985; Weiser et al., 1986; Baret and Guyot, 1991) and subsequently functional relationships using radiative transfer models (Goel and Deering, 1985; Jacquemoud et al., 1995); both of which are now summarized in standard texts (Asrar, 1989; Liang et al., 2012; Loboda et al., 2017; Chen, 2018; Croft and Chen, 2018). Multispectral algorithms based on globally calibrated functional relationships have been used to generate global coarse resolution vegetation biophysical variable products (Knyazikhin et al., 1998; Deng et al., 2006; Baret

* Corresponding author.
E-mail addresses: najib.djamai@canada.ca (N. Djamai), richard.fernandes@canada.ca (R. Fernandes), marie.weiss@inra.fr (M. Weiss), heather.mcnairn@agr.gc.ca (H. McNairn), kalifa.goita@usherbrooke.ca (K. Goïta).

https://doi.org/10.1016/j.rse.2019.03.020
Received 16 October 2018; Received in revised form 29 January 2019; Accepted 16 March 2019
Available online 30 March 2019
0034-4257/

Table 1
Definition of validated vegetation biophysical variables together with target GCOS or SEN4SCI relative (as %) or absolute uncertainty.

Vegetation biophysical variables	Definition	Uncertainty	
		GCOS	SEN4SCI
Leaf area index (LAI)	One half the total green leaf area per unit horizontal ground surface area [m^2/m^2]	15%	Max (20%,1)
Fraction of vegetation cover (fCover)	Green fraction seen from nadir direction [%]	–	0.15
Canopy Water Content (CWC)	Amount of water in canopy foliage [kg/m^2]	–	20%

et al., 2007; Baret et al., 2013; Disney et al., 2016). Similar decametric resolution products are currently not globally available although there are processors capable of global systematic processing, including those developed by the Landsat science team (Ganguly et al., 2012) and the Sentinel-2 Mission (the Simplified Level 2 Product Prototype Processor or SL2P; Weiss and Baret, 2016).

Validation is required to determine if products meet specifications (Baret et al., 2007; Camacho et al., 2013a). This is especially true for products derived using global algorithms since the inverse problem of estimating vegetation biophysical variables from single angle multi-spectral reflectance data is ill-posed in that there is usually no unique solution (Baret and Guyot, 1991; Teillet et al., 1997). The lack of a unique solution together with relatively low signal-to-noise ratios at both high and low LAI levels (Baret and Buis, 2008) results in algorithms that may exhibit high sensitivity (e.g. worse than performance requirements) to typical uncertainties in prior estimates of soil and vegetation variables (Combal et al., 2003).

The Committee of Earth Observing Systems (CEOS), through its Working Group in Calibration and Validation (WGCV), coordinates validation activities of satellite products (CEOS, 2016). A number of validation studies (see for example, Garrigues et al., 2008; Pisek and Chen, 2007; Claverie et al., 2013) have been conducted for coarse ($\geq$250 m) resolution LAI products including many based on standards defined by the CEOS Working Group on Calibration and Validation Land Product Validation subgroup (Fernandes et al., 2014). These studies typically report the accuracy (A) as the sum of differences between matched product and reference estimates (i.e. the bias), the precision (P) as the root mean square difference after subtracting the bias, and the uncertainty (U) as the root mean square difference, following the American National Standards Institute (ANSI/ASME, 1985). While these studies are not yet globally representative or comprehensive across all products they indicate that coarse resolution LAI products frequently have precision errors in excess of the measurement error of input reflectance and bias in excess of 30% for both low ($<$ 1) and high ($>$ 4) LAI.

The validation of decametric resolution biophysical variables products from globally applicable algorithms has typically been performed by producers at a limited ($<$ 30) number of sites and periods (i.e. CEOS LPV Stage 1; e.g. Bacour et al., 2006; Richter et al., 2009). Validation over a broad range of conditions in terms of both sites and stages of the growth cycle (i.e. CEOS LPV Stage 2; e.g. Morisette et al., 2006) is required as algorithms or products with global applicability/coverage become available. Both the Landsat and SL2P algorithms are prime candidates for such validation efforts. Initially we hoped to test both algorithms using standard Landsat Operational Line Imager (OLI) and Sentinel-2 Multispectral Imager (MSI) surface reflectance imagery. Due to resource limitations, the Landsat algorithm was not applied. Instead, we validated the SL2P algorithm when applied to OLI and MSI data.

It is critical to prioritize Stage 2 sampling locations due to limited resources for in-situ measurement. Ideally one would implement a representative randomized sampling design for measurement sites (e.g. BELMANIP, Baret et al., 2006). However, due to resource limitations in-situ networks are currently designed to serve multiple monitoring and validation requirements (e.g. The National Ecological Observatory Network, The Terrestrial Ecosystem Research Network, The Integrated Carbon Observation System and The Joint Experiment for Crop Assessment and Monitoring). Since previous validation studies for vegetation biophysical variables indicate that biases due to prior assumptions in global algorithms are commonplace and large (Camacho et al., 2013a), it is prudent to perform validation over regions where such biases are likely to occur. This corresponds to regions with large spatial and temporal variation in soil and vegetation variables that are also still representative of other areas. Croplands are an obvious example as i) they include a growth cycle with systematic co-variation in variables such as spatial clumping, leaf angle distribution, foliage reflectance, foliage transmittance, and canopy height between crop types and ii) validation results may be transferrable to croplands with similar management practices, varieties and soil conditions.

The lower revisit frequency of decametric versus coarse resolution imagers poses a challenge for Stage 2 validation over croplands due to the larger temporal variation in vegetation variables in comparison to other undisturbed biomes (McNairn et al., 2017). Previously, significant effort was placed in defining good practices for spatial scaling of reference measurements when validating coarse resolution products while temporal scaling was based on either zero or first order interpolation (e.g. Fernandes et al., 2014). Spatial scaling is not a major difficulty when performing validation over crop fields that are relatively large and uniform in comparison to decametric resolution imagery. However, there is a need to develop good practices for comparison of products and reference data that are sparsely sampled in time. Previous studies have used zero-order temporal interpolation (e.g. Weiss et al., 2001; Canisius and Fernandes, 2012; Camacho et al., 2013b) for comparing time series of in-situ and satellite estimates.

In consideration of these issues related to Stage 2 validation of decametric resolution vegetation biophysical variables from global processors applied to decametric resolution imagery, this study addresses two research questions:

1. What is the accuracy, precision and uncertainty of LAI, fCover and CWC products derived from application of the SL2P processor to systematically processed Sentinel-2 MSI and Landsat 8 OLI imagery over a range of crop types through the growing season?
2. How do temporal profiles of LAI, fCover and CWC derived from application of the SL2P processor to Sentinel-2 MSI and Landsat 8 OLI imagery compare with each other and with temporal profiles from in-situ data?

The VALSE2 project has validated the SL2P algorithm in terms of all biophysical variables using MSI imagery simulated using airborne hyperspectral data (Camacho et al., 2013b). While the validation indicated mixed performance, in terms of cropland temporal sampling, it was limited to measurements during single stages in the growing season and it was generally not possible to quantify the uncertainty of the simulated imagery. Delloye et al. (2018) have validated time series of canopy chlorophyll content estimates derived from application of the BV-NET algorithm (Weiss et Baret, 1999) to MSI imagery over croplands. Our study supplements their work by validating time series of multiple vegetation variables simultaneously.

Our study covers the growth season but does not extend further due to the availability of in-situ measurements that were originally taken for a soil moisture product validation experiment (McNairn et al., 2017). The SL2P algorithm theoretical basis document includes

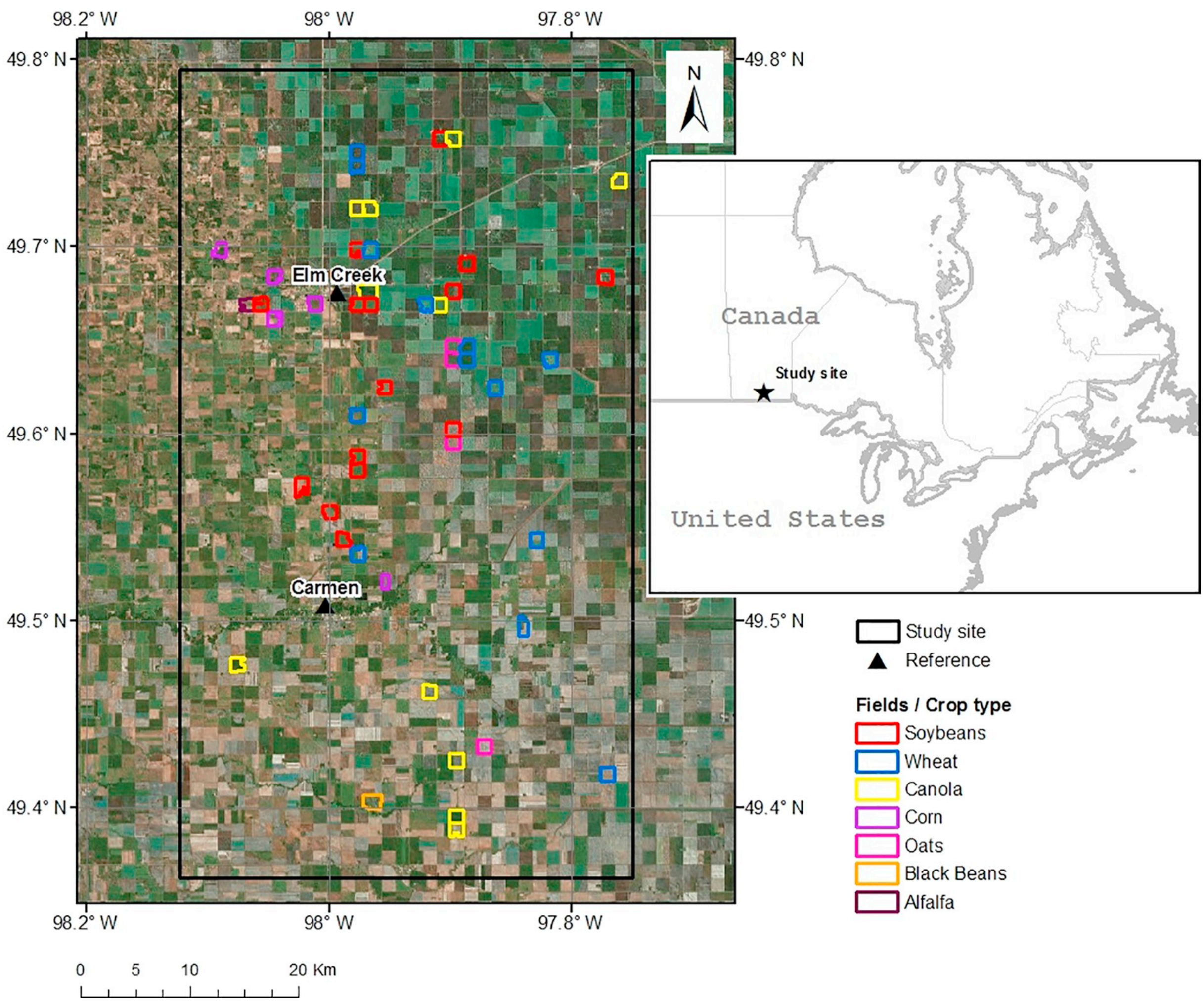

Fig. 1. The SMAPVEX16-MB study site – geographical position, sampled fields and reference place names indicated (Basemap: World Imagery, ESRI)

Table 2
Crop type of plots sampled within theSMAPVEX16-MB study area.

Crop type	Fields	#ESU per field
Soybeans	15	3
Canola	11	3
Wheat	13	3
Corn	5	3
Oats	3	3
Black beans	1	3
Alfalfa	2	3

estimates of expected product uncertainty that indicate that the algorithm should satisfy SEN4SCI specifications when using MSI imagery during the entire growth season (Weiss et al., 2016). As such our null hypothesis is that LAI, fCover and CWC will be derived within the SEN4SCI specification from MSI and OLI imagery (Table 1). We further hypothesize that the use of standard regression analysis tools to determine the appropriate temporal interpolation function will result in comparable uncertainty statistics to those observed for punctual comparisons. In this case, the profiles can be used to provide statistically meaningful comparisons when in-situ and satellite estimates are not coincident.

2. Material

2.1. Study area

The study area of approximately 26 km × 48 km was located in Manitoba, Canada, between the latitudes 49.3°N and 49.8°N and longitudes 97.7°Wand 98.2°W (Fig. 1). The study area was predominantly flat with a mean elevation of 230 m above sea level. Annual crops covered > 90% of the area, while grassland and pasture occupied < 5% of the area; the remaining areas were built up or forested.

2.2. Data Sources

2.2.1. Ground truth data

In-situ measurements of vegetation variables were collected during the SMAP Validation Experiment 2016 in Manitoba (SMAPVEX16-MB; Bhuiyan et al., 2018) between 8th to 20th June and 10th to 22th July 2016. Fifty cropped fields were sampled intermittently during the experiment (Fig. 1 and Table 2). Vegetation biophysical variables, including LAI, fCover and CWC, were measured for three Elementary Sampling Units (ESU) distributed over each field (McNairn et al., 2017). The ~3 m geolocation accuracy of ESUs was substantially smaller than the ESU spatial footprint, so we assume geolocation uncertainty of in-situ measurements has a negligible impact on comparisons. Table 3 presents the in-situ data acquisition dates and ESU number sampled each day for the different biophysical variables.

LAI and fCover were estimated from digital hemispherical

Table 3
Acquisition dates and ESU number sampled each day for the different biophysical variables (DOY indicates day of year).

	ESU number		
DOY	LAI	FCOVER	CWC
165	79	79	44
167	63	63	28
170	64	64	34
172	60	60	27
179	42	42	14
180	44	44	29
187	34	34	19
188	39	39	21
193	76	76	31
194	72	72	29
199	78	78	44
202	62	62	33
203	7	7	7

photographs using CanEye Version 5.1 following the SMAPVEX16-MB protocol (McNairn et al., 2017) that corresponds in turn to the Canada Centre for Remote Sensing (CCRS) protocol for crops (Fernandes et al., 2012). For each ESU, seven downward looking photos were captured from above the canopy using a Digital Hemispheric Photos (DHP) camera with a fish eye lens every 5 m along each of two parallel transects spaced 5 m apart. All 14 photos were processed together to provide one estimate of LAI and fCover per ESU.

Canopy Water Content (CWC) was determined using gravimetric methods (McNairn et al., 2017). One biomass sample was collected at three ESU for each site. For canola, wheat, oats and alfalfa, all above ground biomass was collected by cutting all vegetation at the soil level within a 0.5 m × 0.5 m square placed over the canopy. For corn and beans, 5 plants along two rows were collected. Crop samples were partitioned by plant organs. Wet and dry weights of leaves (leaves + stems) were determined for soybean, canola and corn (wheat and oat). Knowing the crop density (determined for each field during the field campaign), wet and dry weights were scaled to a 1 m × 1 m area. Finally, in-situ CWC, used in this study, was computed by subtracting wet and dry weights of leaves (for soybean, canola and corn) or of leaves + stems (for wheat and oat).

2.2.2. Satellite data

2.2.2.1. Sentinel-2/MSI. Sentinel-2 is a constellation of satellites, Sentinel-2A and Sentinel-2B, launched by the European Space Agency (ESA) on 23 June 2015 and 7 March 2017, respectively (European Space Agency, 2012). They occupy the same sun-synchronous orbit at an altitude ~786 km but separated by 180°. Together, they provide better than 5-day revisit of the Earth's land surfaces with an equatorial overpass time at approximately10:30 a.m. (descending node). Sentinel-2A and Sentinel-2B carry a virtually identical decametric resolution Multi-Spectral Imager (MSI) covering the visible, the near infrared (NIR) and the shortwave-infrared (SWIR) spectral regions (Table 4; Drusch et al., 2012).

2.2.2.2. Landsat-8/OLI. Landsat-8 is part of the Landsat Data Continuity Mission (Irons et al., 2012), launched on February 11, 2013. Landsat-8 has a sun-synchronous orbit at an altitude of ~705 km, with approximately 16-day revisit of the Earth and an equatorial overpass time of approximately10:15 a.m. (descending node). Landsat-8 carries the Operational Land Imager (OLI, Knight and Kvaran, 2014) that has eight spectral bands at 30 m spatial resolution covering the visible, the near infrared (NIR) and the shortwave-infrared (SWIR) spectral regions, and one 15 m spatial resolution panchromatic band (Table 5).

Table 4
Sentinel-2/MSI bands (bands used by SL2P are indicated in bold).

Sentinel-2/MSI Bands	Central Wavelength (μm)	Resolution (m)
Band 1 – Ultra Blue (coastal/aerosol)	0.443	60
Band 2 – Blue	0.490	10
Band 3 – Green	**0.560**	**10**
Band 4 – Red	**0.665**	**10**
Band 5 – Vegetation Red Edge	**0.705**	**20**
Band 6 – Vegetation Red Edge	**0.740**	**20**
Band 7 – Vegetation Red Edge	**0.783**	**20**
Band 8 – Near Infrared (NIR)	0.842	10
Band 8A – Narrow NIR	**0.865**	**20**
Band 9 – Water vapour	0.945	60
Band 10 – Cirrus	1.375	60
Band 11 – Shortwave Infrared 1 (SWIR 1)	**1.610**	**20**
Band 12 – Shortwave Infrared 2 (SWIR 2)	**2.190**	**20**

Table 5
Landsat-8/OLI bands (bands used by SL2P are indicated in bold).

Landsat 8/OLI bands	Central wavelength (μm)	Resolution (m)
Band 1 - Ultra Blue (coastal/aerosol)	0.443	30
Band 2 - Blue	0.482	30
Band 3 - Green	**0.561**	**30**
Band 4 - Red	**0.655**	**30**
Band 5 - Near Infrared (NIR)	**0.865**	**30**
Band 6 - Shortwave Infrared 1 (SWIR 1)	**1.609**	**30**
Band 7 - Shortwave Infrared 2 (SWIR 2)	**2.201**	**30**
Band 8 - Panchromatic	0.590	15
Band 9 - Cirrus	1.373	30

3. Methodology

3.1. Satellite data preprocessing

MSI L1C data (MSIL1C) covering the study site (granule tiles T14UNA and T14UNV) acquired from June 1st, 2016 to September 30th, 2016 were downloaded from the Copernicus Open Access Hub. Twelve acquisition dates with cloud free coverage of some ESUs were available for each granule tile (Table 6). The Sen2Cor processor (Version 2.4.0, Mueller-Wilm et al., 2017) was used to convert MSIL1C data

Table 6
Acquisition dates and the cloud fraction for the used MSI and OLI images (DOY indicates day of year).

MSI			OLI			
	Cloud fraction (%)			Cloud fraction (%)		
DOY	T14UNA	T14UNV	DOY	031025	031026	032025
162	1	0	159	–	–	71
165	1	16	168	88	–	–
172	1	13	175	–	–	0
175	1	14	184	38	52	–
202	66	14	191	–	–	80
212	2	1	200	2	2	–
215	1	19	207	–	–	0
235	1	20	216	67	63	–
242	4	0	223	–	–	0
245	11	34	232	56	67	–
252	0	0	239	–	–	34
272	4	3	264	0	0	–
			271	–	–	64

to atmospherically corrected top-of-canopy (TOC) reflectance data (MSIL2A). MSI 10-m spatial resolution bands were resampled to match the 20 m grid using the nearest method integrated in the Sentinel Application Platform (SNAP).

OLI TOC data (OLIL2) covering the study site (granule tiles 031025, 031026 and 032025) acquired from June 1st, 2016 to September 30th, 2016 were downloaded from the United States Geological Survey (USGS; https://espa.cr.usgs.gov/). The data had been corrected for atmospheric effects using the Landsat Surface Reflectance Code (LaSRC). Thirteen acquisition dates with cloud free coverage of some ESUs were available (Table 6).

The scene classification map (quality assurance layer) produced by Sen2Cor (LaSRC) was used to mask cloudy pixels in MSIL2A (OLIL2) imagery. Visual examination of each image found that the masks had negligible commission errors over the study sites. MSIL2A and OLIL2 data were clipped according to the area extension for the study area. Geo-referencing quality assessment of both MSIL2A and OLIL2 images was performed using the local road network provided by the Government of Canada GeoGratis platform. A geolocation error less than one pixel was observed in the vicinity of the ESUs for both sensors. Quality assessment of MSI and OLI surface reflectance estimates indicate that the bands used by the SL2P algorithm have typical accuracy, precision, and uncertainty less then ~5% over flat vegetated terrain (Markham et al., 2014; Morfitt et al., 2015; Djamai and Fernandes, 2018; Doxani et al., 2018).

3.2. Vegetation biophysical variables estimation using SL2P

The Simplified Level 2 Product Prototype Processor (SL2P) algorithm (Weiss et al., 2016) was used to derive vegetation biophysical variables from MSIL2A and OLIL2 reflectance data. SL2P was developed to systematically retrieve vegetation biophysical variables from Sentinel-2/MSI data. It was implemented within the Sentinel Application Platform (SNAP) for processing MSI data. The algorithm used within the SL2P processor was used for processing OLI data (personal communication with Marie Weiss, INRA).

SL2P is a collection of backpropagation artificial neural networks (ANN) trained using a globally representative set of simulations from a canopy radiative transfer (RT) model (PROSAILH: PROSPECT (Jacquemoud and Baret, 1990) + SAILH (Verhoef, 1984)). PROSAILH computes the reflectance in the entire spectral domain as well as fCover and fAPAR using (1) leaf optical properties (leaf water content (Cw), leaf chlorophyll content, leaf brown pigments content, and the PROSPECT leaf structure parameter), (2) canopy structure (LAI, average leaf angle, hot spot parameter, and soil brightness), (3) the background reflectance spectrum and (4) the geometrical configuration of illumination and observation (i.e. the solar and view zenith angles, and the solar-view relative azimuthal angle). Simulations were sampled from a single joint probability density function of canopy variables, based on heuristics considered representative of cropland and natural vegetation, and a regular sampling of local flat earth view and illumination geometry for the global coverage of the sensor under consideration. The same set of simulations were used to calibrate all neural networks developed for a given sensor. Two neural networks were trained for each of LAI, CWC and fCover. The first neural network was trained to predict the expected value of the biophysical variable given TOC reflectance (Tables 4 and 5) and acquisition geometry. The second neural network was trained to predict the residual of the estimated biophysical variable by the first neural network.

3.3. Vegetation biophysical variables estimation using locally calibrated VI models

Validation studies have often found evidence of local bias with estimates from global vegetation biophysical variables retrieval algorithms (Weiss et al., 2007; Garrigues et al., 2008; Garcia-Haro et al., 2018). This prompts the question as to whether these biases are due to issues with the retrieval algorithm and measurement error or actually due to limited information within canopy reflectance. One approach to address this question is to evaluate, in parallel with global retrieval algorithms, locally calibrated algorithms applied to the same TOC data that depend only on structural (e.g. statistical regression) relationships with in-situ measurements (Garrigues et al., 2008; Abuelgasim et al., 2006). Here, LAI, fCover and CWC were also estimated using empirical vegetation indices (VI) based on separate regression models between either MSIL2A (MSI/VI) or OLIL2 (OLI/VI) data and matching in-situ reference measurements. A 3-fold cross-validation technique (Snee, 1977) was used to calibrate each model. The objective was to produce the best performing unbiased biophysical variables estimates using a locally calibrated method for comparison with estimates from the SL2P algorithm applied to the same data. The dataset was randomly divided into 3 equal-sized sub-datasets. Two sub-datasets are selected for calibration and a single sub-dataset is used for validation. The cross-validation process is repeated 3 times, with each of the 3 sub-datasets used as a cross-validation dataset. Thereby, all in-situ reference data were used for both calibration and cross-validation of the VI based estimates, and each single observation is used for cross-validation exactly once.

The performance of structural regression models depends on the choice of the regression function both in terms of satisfying assumptions regarding regression and prediction uncertainty (Fernandes and Leblanc, 2005). Since the goal of the regression model here is to quantify the potential performance of a locally calibrated algorithm a number of univariate models were developed using different vegetation indices known to be related to the desired biophysical quantity. This approach represents an ensemble of estimates rather than the best possible estimate that may vary by image, crop type, based on arbitrary band combinations. Four VI models were tested (Table 7). NDVI and NDWI are extensively applied vegetation indices related to vegetation biophysical variables (Ceccato et al., 2002; Zarco-Tejeada et al., 2003; Jackson et al., 2004). In this study, NDWI was computed from both SWIR 1 band (NDWI_1) and SWIR 2 band (NDWI_2). Verrelst et al. (2015) demonstrated that 3BSI vegetation index performs the best to empirically estimate LAI from simulated MSI data when compared to all possible band combinations for two- and three-band index formulations. Regarding the selected fitting function, results from linear and exponential models were also inter-compared. Only results from the best performing regression model, in terms of cross-validation error, were presented and discussed.

3.4. Validation strategy

Validation was performed in two steps. In the first step, punctual comparisons were performed between in-situ measurements and spatially co-located SL2P estimates acquired within ± 1 day. Due to differences between MSI and OLI cloud-free acquisition dates (Table 6), there were insufficient dates to provide a statistically meaningful validation of MSI/SL2P and OLI/SL2P estimates using the same combination of ESUs and dates. Rather, in-situ data from four acquisition dates

Table 7
Used vegetation indices models.

Vegetation indices model name	Vegetation indices model equation	Reference
Modified Simple Ratio (RSR)	$\frac{(NIR/Red)-1}{\sqrt{(NIR/Red)+1}}$	Chen, 1996
Normalized Difference Vegetation Index (NDVI)	$\frac{NIR-Red}{NIR+Red}$	Rouse et al., 1974
Normalized Difference Water Index (NDWI)	$\frac{NIR-SWIR}{NIR+SWIR}$	Gao, 1996
Enhanced Vegetation Index (EVI)	$\frac{2.5\,(NIR-Red)}{NIR+6Red-7.5\,Blue+1}$	Liu et al., 1995

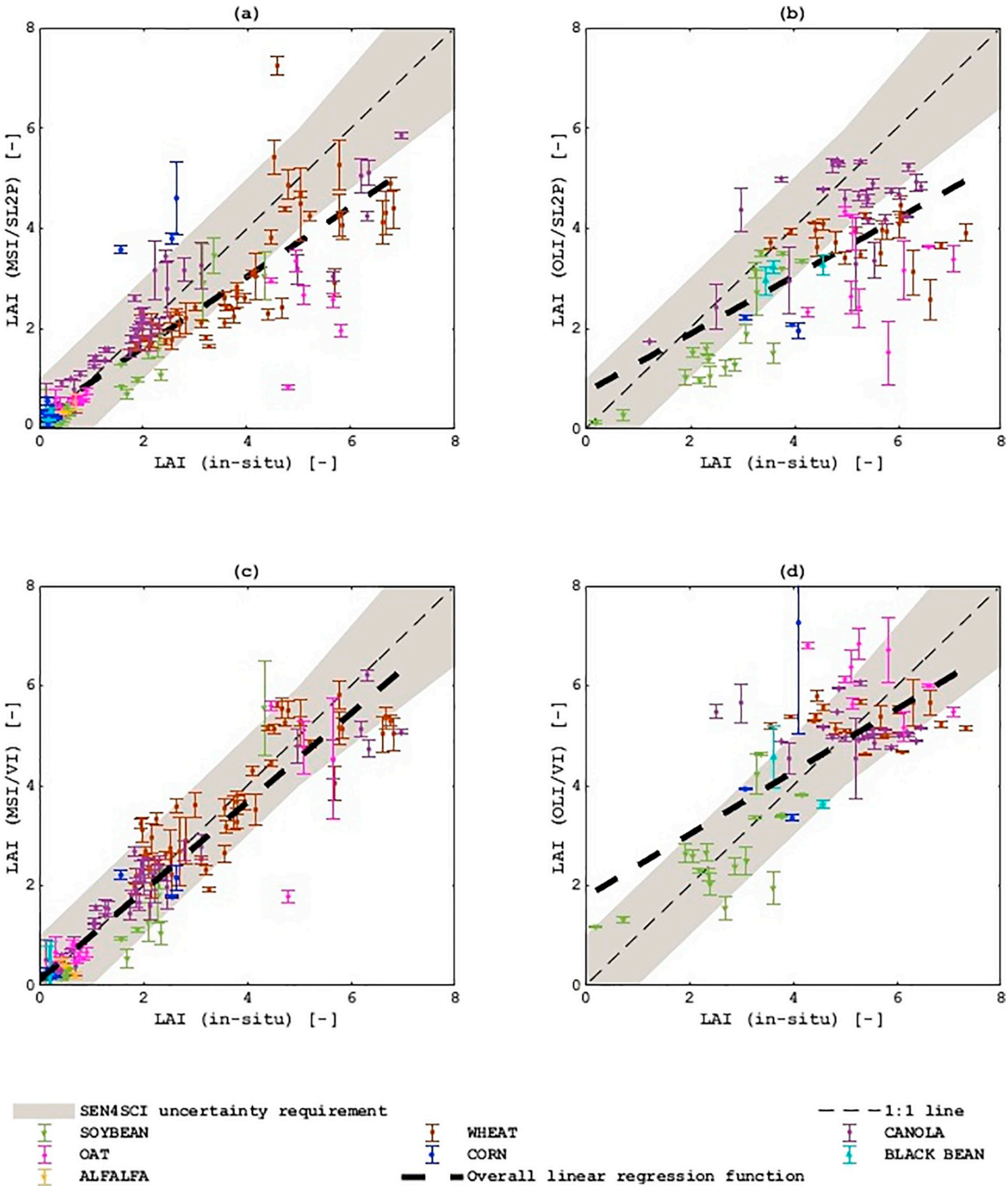

Fig. 2. Scatter plot and overall linear regression function between in-situ measurements of LAI and estimates from (a) MSI/SL2P, (b) OLI/SL2P, (c) MSI/VI and (d) OLI/VI: the gray area presents the SEN4SCI uncertainty requirement.

(DOY 165, 172, 202, 203) were used to validate MSI/SL2P estimates, and in-situ data from two acquisition dates (DOY 167, 199) were used to validate estimates from OLI/SL2P.

SL2P estimates from one-day shifted acquisitions were interpolated using a polynomial temporal transfer function. Notwithstanding the fact that the fields were qualitatively uniform in the vicinity of each ESU, the mean and standard deviation of SL2P estimates from 3 × 3 pixels around the ESU centre was recorded to account for local spatial variation in variables. For all data and also for each crop type, the RMSE and bias between in-situ measurements and SL2P estimates was computed to estimates of total uncertainty and accuracy respectively. Only statistics corresponding to > 5 samples were reported to ensure they were sufficiently precise. Ideally, performance statistics should be presented as a function of magnitude of the validated variable (e.g. Fernandes et al., 2014; Doxani et al., 2018). However, the sampling distributions within the validation datasets were not sufficiently large or representative. Instead, the linear slope between estimated and reference quantities was used to indicate how bias is distributed as a function of variable level and the Uncertainty Agreement Ratio (UAR [%], the percentage of estimates falling within the SEN4SCI uncertainty presented in Table 1) was computed to provide an estimate of uncertainty with reduced sensitivity to the range of sampled variables. As

Table 8
Validation statistics between in-situ measurements of LAI and estimates from MSI/SL2P, OLI/SL2P, MSI/VI and OLI/VI. Slopes significantly different from 0 at *p*-value equal to 0.05 are noted by (✓).

Model	Crop type	MSI						OLI					
		RMSE [-]	UAR [%]	Bias [-]	Slope	N	Range [-]	RMSE [-]	UAR [%]	Bias [-]	Slope	N	Range [-]
SL2P	Soybean	0.38	96	−0.19	0.75 (✓)	54	4.33	0.97	61	−0.80	0.93 (✓)	18	3.88
	Wheat	1.27	58	−0.85	0.68 (✓)	48	4.97	1.99	24	−1.66	−0.09	21	3.76
	Canola	0.77	90	−0.08	0.67 (✓)	39	6.85	1.13	64	−0.66	0.50 (✓)	25	5.26
	Oat	1.84	60	−1.14	0.40 (✓)	15	5.57	2.73	11	−2.52	0.17	9	2.50
	Corn	0.83	80	0.40	1.78 (✓)	15	2.44	–	–	–	–	3	–
	Black Bean	–	–	–	–	2	–	–	–	–	–	3	–
	Alfalfa	–	–	–	–	3	–	–	–	–	–	0	–
	Overall	***0.98***	***80***	***-0.37***	***0.70 (✓)***	***176***	***6.98***	***1.63***	***44***	***−1.21***	***0.59 (✓)***	***79***	***7.14***
VI	Soybean	0.75	91	0.05	1.37 (✓)	53	4.33	0.63	83	0.06	0.80 (✓)	18	3.88
	Wheat	0.74	90	−0.09	0.72 (✓)	48	4.97	0.89	76	−0.11	0.13	21	3.76
	Canola	0.49	95	−0.08	0.84 (✓)	39	6.85	1.10	79	−0.18	−0.08	24	4.03
	Oat	1.02	85	−0.18	0.87 (✓)	13	5.40	0.93	78	−0.01	−0.17	9	2.50
	Corn	0.45	87	−0.12	0.61 (✓)	15	2.44	–	–	–	–	3	–
	Black Bean	–	–	–	–	2	–	–	–	–	–	2	–
	Alfalfa	–	–	–	–	3	–	–	–	–	–	1	–
	Overall	***0.69***	***91***	***−0.05***	***0.92 (✓)***	***173***	***6.98***	***0.95***	***79***	***−0.04***	***0.65 (✓)***	***77***	***7.14***

CWC specifications were not available, a performance requirement of uncertainty $\leq 0.20\,kg/m^2$ for CWC values lower than $1\,kg/m^2$ corresponding to a prior estimated uncertainty from the SL2P algorithm (Weiss et al., 2016) was used. Products were also compared to biophysical variable estimates derived by applying VI models to MSIL2A and OLIL2 images.

In a second step, temporal profiles of biophysical variables derived from MSI/SL2P and OLI/SL2P as well as in-situ measurement data were inter-compared. For each dataset, the mean and standard deviation values of each biophysical variable and in-situ data measurement day were computed for the different crop-types. Then, a third-degree polynomial function was used to fit the temporal profiles based on the maximum explained variance and the reliability of obtained temporal profiles (assessed qualitatively). Logistics functions were not used to avoid additional constraints on the comparison of profiles. The RMSE and bias between the temporal profiles of SL2P estimates and in-situ measurements were computed. In addition, the coefficient of determination (R^2) was added for this analysis as a metric of the similarity of the shape of the temporal profiles.

4. Results

4.1. Validation of biophysical variables

4.1.1. Leaf area index (LAI)

Fig. 2 (Table 8) shows punctual comparisons of ESU LAI estimates derived using MSI/SL2P, OLI/SL2P, MSI/VI and OLI/VI with in-situ measurements. Although, multiple VI performed similarly well, the NDWI_1 based VI model performed better when compared to empirically retrieved LAI. This VI had the lowest RMSE amongst all assessed VI models for all crop types (see Section 3.3). Consequently, only results from the NDWI_1 based VI model were presented.

In terms of LAI accuracy, Fig. 2a and b indicate that, considering all crop types, both MSI/SL2P and OLI/SL2P systematically underestimated in-situ LAI. In each case, the underestimation corresponded to both a slope < 1 (significantly different from 0 at $p = .05$) and a negative bias (slope = 0.70, bias = −0.37 for MSI/SL2P and slope = 0.59, bias = −1.21 for OLI/SL2P). Crop-type specific comparisons for MSI/SL2P indicated (statistically significant) slopes < 1 except for corn which was overestimated substantially for LAI > 1. Crop-type specific estimates of slope for OLI/SL2P (< 1 like estimates from MSI/SL2P) were statistically reliable only for soybean and canola.

In terms of LAI uncertainty, Table 8 indicates that over all crop types, the RMSE between estimates and in-situ measurements was 0.98 using MSI/SL2P (80% of estimates meet the SEN4SCI uncertainty requirements) and 1.63 using OLI/SL2P (only 44% of estimates meet the SEN4SCI uncertainty requirements). MSI/SL2P has a lower RMSE (< 0.83) and higher UAR (> 80%) for soybean and canola in comparison to oat (RMSE =1.84, UAR = 60%) and wheat (RMSE = 1.27, UAR = 58%). While OLI/SL2P showed a similar pattern as a function of crop type it was consistently worse in terms of both RMSE and UAR with a best case RMSE (UAR) of 0.97 (61%) obtained for soybean.

As expected, better LAI uncertainty metrics are generally observed for MSI/VI and OLI/VI (Fig. 2c and d) in comparison to respective MSI/SL2P and OLI/SL2P estimates. The RMSE between estimates and in-situ measurements was 0.69 using MSI/VI (compared to 0.98 using MSI/SL2P) and 0.95 using OLI/VI (compared to 1.63 using MSI/SL2P). Moreover, the overall uncertainty agreement ratio was 91% for MSI/VI (compared to 80% using MSI/SL2P) and 79% for OLI/VI (compared to 44% using OLI/SL2P). Accuracy for VI based estimates cannot be directly assessed by the slope in comparison to reference measurements since the VI algorithms were calibrated by unbiased regression estimators using the same reference data.

4.1.2. Vegetation fraction cover (fCover)

Fig. 3 (Table 9) compares fCover estimates derived using MSI/SL2P, OLI/SL2P, MSI/VI and OLI/VI with in-situ measurements. MSI/VI and OLI/VI products were obtained using an NDVI model as it had the lowest RMSE in comparison to the other assessed VI models for all crop types (see Section 3.3).

In terms of fCover accuracy, Fig. 3a and b show that both MSI/SL2P and OLI/SL2P performed well when considering all crops. This conclusion is supported by the observation that the linear regressions versus in-situ measurements closely follow the 1:1 line for MSI/SL2P

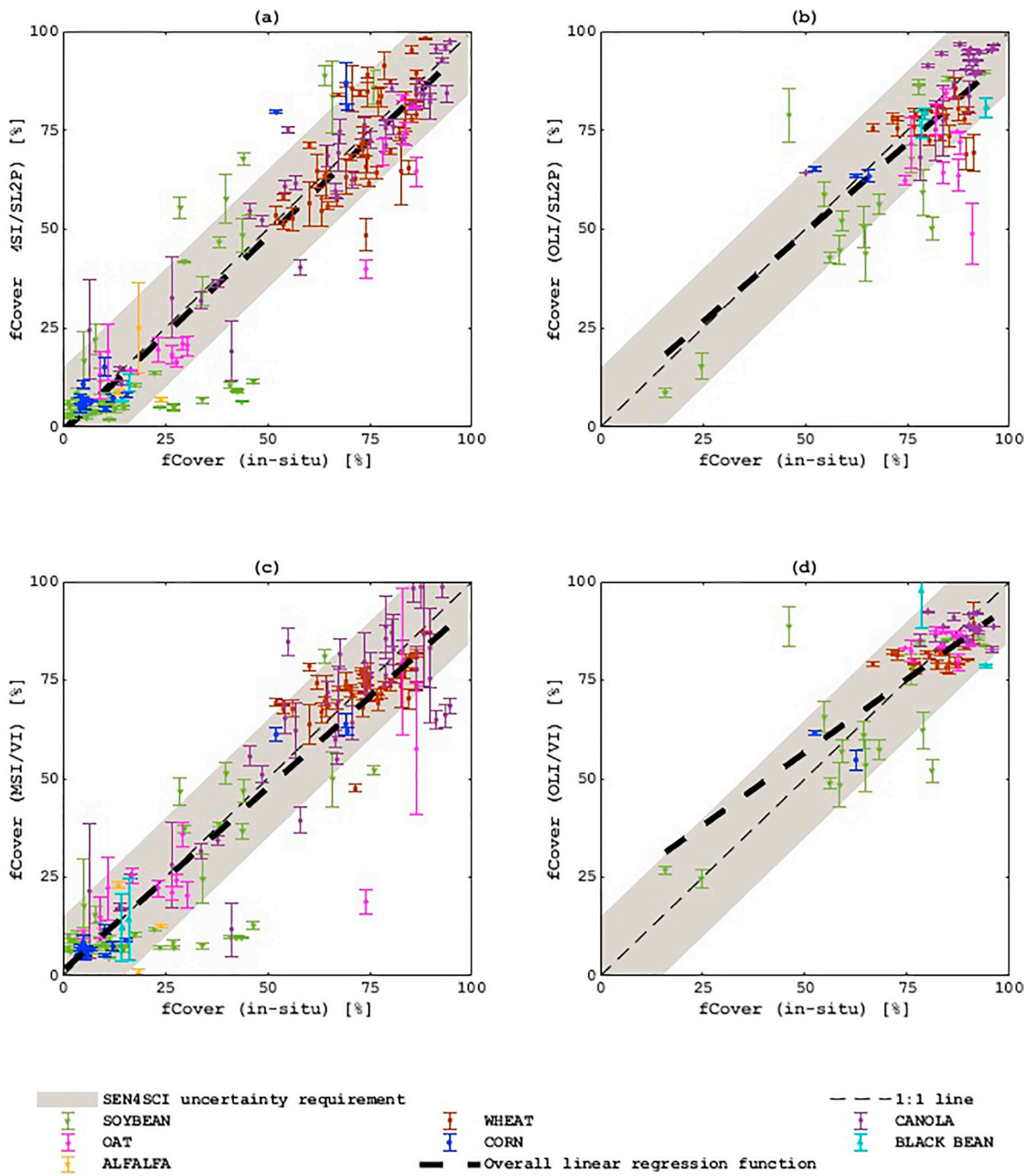

Fig. 3. Scatter plot and overall linear regression function between in-situ measurements of fCover and estimates from (a) MSI/SL2P, (b) OLI/SL2P, (c) MSI/VI and (d) OLI/VI: the gray area presents the SEN4SCI uncertainty requirement.

(slope = 0.99, bias = −1.84%) and OLI/SL2P (slope = 0.93, bias = −3.75%). Crop specific accuracy statistics showed increased variation with (statistically significant) slopes < 1 for oat (0.83) using MSI/SL2P and for canola using OLI/SL2P (0.77) and slopes > 1 for corn using MSI/SL2P (1.30).

In terms of fCover uncertainty, the RMSE between all in-situ measurements and estimates from MSI/SL2P was 11.39% (84% of estimates meet the SEN4SCI uncertainty requirements). Very similar levels of uncertainty were observed for OLI/SL2P with an RMSE between in-situ measurements and estimates from OLI/SL2P of 10.95% (87% of estimates meet the SEN4SCI uncertainty requirements). The worst-case crop varied by algorithm with soybean presenting the highest RMSE and the lowest uncertainty agreement ratio (RMSE = 14.66%, UAR = 75%) using MSI/SL2P, and oat presents the highest RMSE and the lowest uncertainty agreement ratio using OLI/SL2P (RMSE = 17.49%, UAR = 56%).

Fig. 3c and d compare fCover estimates derived using MSI/VI and OLI/VI with in-situ estimates. For both MSI and OLI, the VI estimates had similar uncertainty to their corresponding SL2P estimates.

4.1.3. Canopy Water Content (CWC)

Fig. 4 (Table 10) compares CWC estimates derived using MSI/SL2P, OLI/SL2P, MSI/VI and OLI/VI with in-situ measurements. MSI/VI and OLI/VI CWC products were derived using the NDWI_1 model as it had

Table 9
Validation statistics between in-situ measurements of fCover and estimates from MSI/SL2P, OLI/SL2P, MSI/VI and OLI/VI. Slopes significantly different from 0 at *p*-value equal to 0.05 are noted by (✓).

Model	Crop type	MSI						OLI					
		RMSE [%]	UAR [%]	Bias [%]	Slope	N	Range [%]	RMSE [%]	UAR [%]	Bias [%]	Slope	N	Range [%]
SL2P	Soybean	14.66	75	−2.71	0.97 (✓)	55	76	15.05	78	−4.89	0.96 (✓)	18	74
	Wheat	9.61	90	−1.12	0.88 (✓)	48	37	8.81	90	−4.34	-0.03	21	22
	Canola	8.02	90	−1.06	0.92 (✓)	39	88	5.57	100	0.78	0.77 (✓)	25	47
	Oat	12.40	87	−7.34	0.83 (✓)	15	81	17.49	56	−14.15	0.22	9	13
	Corn	9.82	87	3.78	1.30 (✓)	15	66	–	–	–	–	3	–
	Black Bean	–	–	–	–	2	–	–	–	–	–	3	–
	Alfalfa	–	–	–	–	3	–	–	0	–	–	0	–
	Overall	11.39	84	−1.84	0.99 (✓)	177	94	10.95	87	−3.75	0.93 (✓)	79	81
VI	Soybean	13.79	80	−3.43	0.63 (✓)	54	76	14.41	78	0.40	0.77 (✓)	18	74
	Wheat	9.13	94	−0.91	0.27 (✓)	48	37	8.07	95	−1.56	−0.22	20	22
	Canola	13.91	77	−1.19	0.78 (✓)	35	88	5.99	100	−2.20	0.00	24	20
	Oat	19.24	83	−6.66	0.53 (✓)	12	81	4.80	100	0.33	0.03	9	13
	Corn	5.59	100	0.13	0.99 (✓)	15	66	–	–	–	–	3	–
	Black Bean	–	–	–	–	2	2	–	–	–	–	2	–
	Alfalfa	–	–	–	–	3	10	–	–	–	–	1	–
	Overall	12.52	85	−2.20	0.90(✓)	169	94	9.48	91	−0.80	0.74 (✓)	76	81

the lowest RMSE in comparison to the other assessed VI models for all crop types (see Section 3.3).

Fig. 4a and b show a considerable scatter of the data for each sensor. In terms of CWC accuracy, both MSI/SL2P and OLI/SL2P systematically underestimate in-situ measurements considering all crop types. For either sensor, the underestimates corresponded to both a slope < 1 (significantly different from 0 at $p = .05$) and a negative bias (slope = 0.42, bias = $-0.37\,kg/m^2$ for MSI/SL2P and slope = 0.24, bias = $-0.23\,kg/m^2$ for OLI/SL2P). Crop specific accuracy statistics also showed an underestimation, except for soybean (bias = $0.12\,kg/m^2$, slope = 1.13) and canola (bias = $1.01\,kg/m^2$, slope not statistically significant) using OLI/SL2P. In comparison to other crops, soybean showed lower biases and slopes closer to 1 for both MSI/SL2P (bias = $-0.04\,kg/m^2$, slope = 0.78) and OLI/SL2P (bias = $-0.12\,kg/m^2$, slope = 1.13). Low bias ($-0.4\,kg/m^2$) and relatively high slope were also obtained for corn using MIS/SL2P. However, high negative biases ($\leq -0.30\,kg/m^2$) joined with low slopes (≤ 0.36) were obtained for wheat and oat irrespective to the sensor.

In terms of CWC uncertainty, the RMSE between CWC estimates and in-situ data across all crops was $0.66\,kg/m^2$ for MSI/SL2P (34% of estimates meet SEN4SCI accuracy requirements) and $0.96\,kg/m^2$ for OLI/SL2P (45% of estimates meet SEN4SCI accuracy requirements). Soybean represents the lowest RMSE value and the highest UAR for both MSI/SL2P (RMSE = $0.07\,kg/m^2$; UAR = 100%) and OLI/SL2P (RMSE = $0.14\,kg/m^2$; UAR = 83%). Low RMSE ($0.14\,kg/m^2$) and high UAR (80%) were also obtained for corn using MSI/SL2P. However, high RMSE ($\geq 0.42\,kg/m^2$) and low UAR ($\leq$63%) values were obtained for wheat, oat and canola irrespective to the sensor.

Fig. 4c and d show CWC estimates obtained using MSI/VI and OLI/VI compared to in-situ measurements. As expected, better uncertainty metrics are obtained using MSI/VI (RMSE = $0.48\,kg/m^2$, UAR = 58%) and OLI/VI (RMSE = $0.61\,kg/m^2$, UAR = 71%) in comparison respectively to metrics obtained for MSI/SL2P (RMSE = $0.66\,kg/m^2$, UAR = 34%) and OLI/SL2P (RMSE = $0.96\,kg/m^2$, UAR = 45%).

4.2. Analysis of MSI/SL2P vegetation biophysical variables time series

Fig. 5 compares temporal profiles based on in-situ measurements, with temporal profiles based on either MSI/SL2P or OLI/SL2P estimates of each biophysical variable as a function of crop type. Error bars represents the mean and the standard deviation of the punctual in-situ measurements over all ESUs for a given crop type and date, and black dashed lines represents the one-sigma confidence intervals of in-situ temporal profiles. Table 11 provides the number (minimum – maximum) of sampled in-situ data (ESU number) for a given crop-type and biophysical variable, as well as statistics between (1) interpolated in-situ data and MSI/SL2P, (2) interpolated in-situ data and OLI/SL2P, and (3) MSI/SL2P and OLI/SL2P time series. APU statistics were not derived for comparisons of interpolated MSI/SL2P or OLI/SL2P time series and in-situ data (punctual or interpolated) since this would implicitly include a smoothing of errors during interpolation that would reflect the temporal sampling distribution of our experiment that may not be representative of conditions generally for the sampled crops.

The relevance of the comparisons between temporal profiles depends on the confidence intervals and representativeness of the interpolated in-situ time series. For the different variables, the mean magnitude of these confidence intervals (0.93 for LAI, 12.93% for fCover and $0.4\,kg/m^2$ for CWC) was generally comparable to the punctual standard deviation of in-situ measurements for all crop types except oat. This suggests that temporal interpolation results in a precision similar to natural spatial variation between fields that is already assumed acceptable for applying the punctual validation results to other regions. In terms of representativeness, although the in-situ measurement temporal profiles only cover a short period (~40 day; from DOY 165 to DOY 203) compared to the entire study period (120 days), they occupy nearly the full vegetation-growing period with the exception of corn. In fact, SMAPVEX16-MB specifically targeted two intensive observing periods with the first period capturing early growth stage following leaf emergence and the second period corresponding to maximum green biomass (McNairn et al., 2017). Consequently, in-situ LAI time series increases for the different crop types from low values (< 2 units) before ~ DOY 170 to higher values (up to 7 units) observed after ~DOY 190.

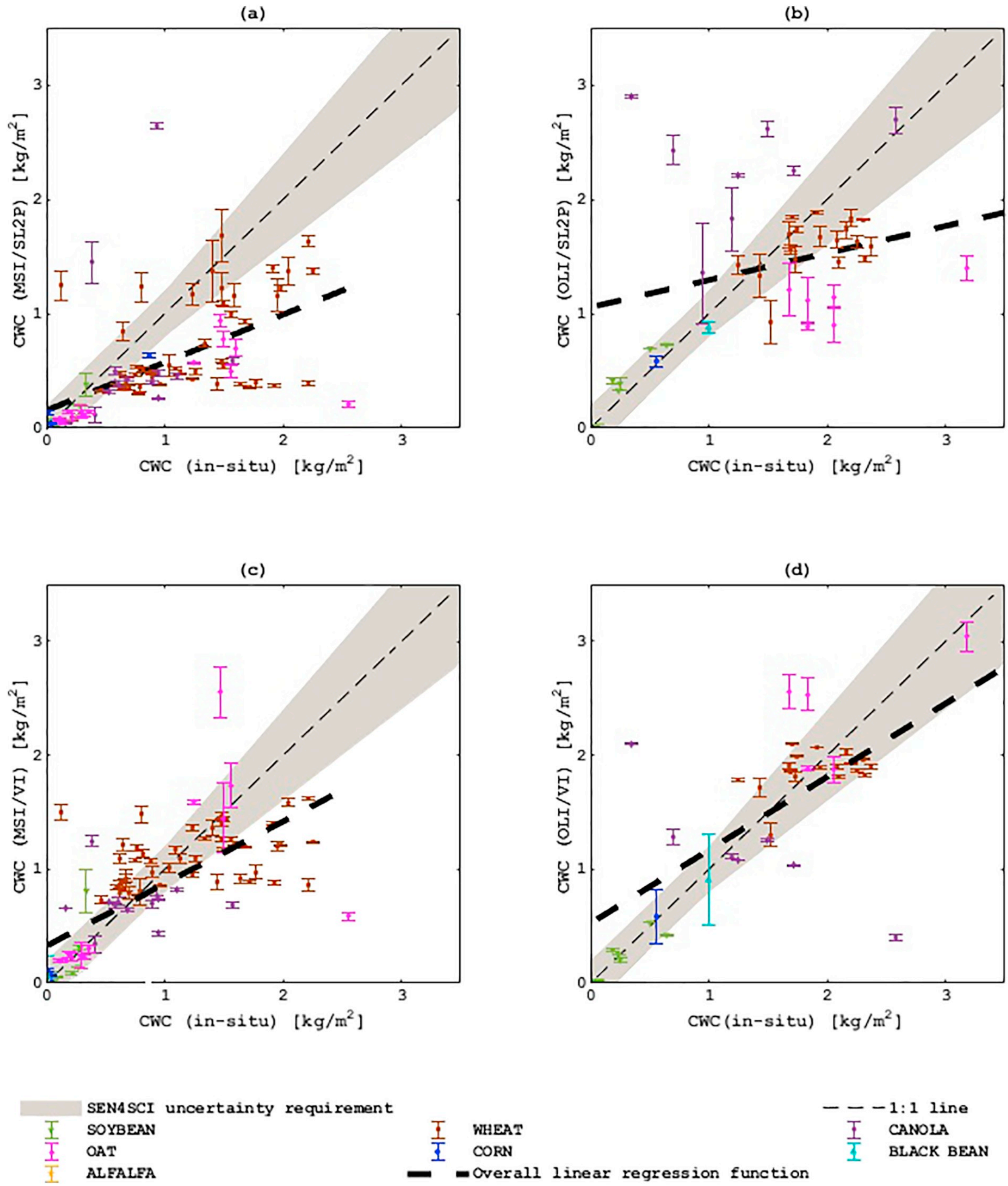

Fig. 4. Scatter plot and overall linear regression function between in-situ measurements of CWC and estimates from (a) MSI/SL2P, (b) OLI/SL2P, (c) MSI/VI and (d) OLI/VI: the gray area presents the SEN4SCI uncertainty requirement.

Similar temporal patterns were generally observed for in-situ fCover and in-situ CWC time series.

Using the R^2 as a metric of the agreement of profile shapes, both MSI/SL2P ($R^2 \geq 0.85$, except for wheat using CWC data) and OLI/SL2P ($R^2 \geq 0.53$, except for wheat using CWC data) showed good agreement with profiles based on in-situ measurements. The RMSE (bias) was below 1.30 (1.22) for LAI and 11.56% (7.34%) for fCover irrespective of sensor when using SL2P. For CWC, the RMSE (bias) was below 0.08 kg/m^2 (0.07 kg/m^2) for soybean and corn. However, an important overestimation (underestimation) was noted for canola (wheat): RMSE (bias) $\geq$0.68 kg/m^2 (0.35 kg/m^2) for canola and $\approx$0.67 kg/m^2 ($-$0.62 kg/m^2) for wheat, irrespective to the sensor.

Additionally, MSI/SL2P and OLI/SL2P time series show high temporal correlation between themselves ($R^2 \geq$ 94 irrespective of biophysical variable) and RMSE (bias) below 0.99 (0.89) for LAI, 12.63% (8.89%) for fCover and 0.32 kg/m^2 (0.31 kg/m^2) for CWC.

5. Discussion

In this study, in-situ data acquired during the SMAPVEX16-MB field campaign were used to validate SL2P estimates of biophysical variables from Sentinel-2/MSI and Landsat-8/OLI data over an agricultural site

Table 10
Validation statistics between in-situ measurements of CWC and estimates from MSI/SL2P, OLI/SL2P, MSI/VI and OLI/VI. Slopes significantly different from 0 at p-value equal to 0.05 are noted by (✓).

Model	Crop type	MSI						OLI					
		RMSE [kg/m²]	UAR [%]	Bias [kg/m²]	Slope	N	Range [kg/m²]	RMSE [kg/m²]	UAR [%]	Bias [kg/m²]	Slope	N	Range [kg/m²]
SL2P	Soybean	0.07	100	−0.04	0.78 (✓)	13	0.31	0.14	83	0.12	1.13 (✓)	6	0.59
	Wheat	0.71	15	−0.51	0.36 (✓)	48	2.12	0.42	63	−0.3	0.3	19	1.12
	Canola	0.71	15	−0.13	0.31	13	1.42	1.25	13	1.01	0.09	8	2.24
	Oat	0.83	38	−0.55	0.25 (✓)	13	2.45	1.64	0	−1.45	0.24 (✓)	9	2.88
	Corn	0.14	80	−0.04	0.68 (✓)	5	0.86	–	–	–	–	1	–
	Black Bean	–	–	–	–	1	–	–	–	–	–	1	–
	Alfalfa	–	–	–	–	0	–	–	–	–	–	0	–
	Overall	0.66	34	−0.37	0.42 (✓)	93	2.55	0.96	45	−0.23	0.24 (✓)	44	4.5
VI	Soybean	0.15	92	0.02	1.44 (✓)	13	0.31	0.1	83	−0.02	0.70 (✓)	6	0.59
	Wheat	0.5	46	−0.11	0.18 (✓)	48	2.12	0.3	79	−0.03	0.19	19	1.12
	Canola	0.43	46	−0.05	0.02	13	1.42	1.12	38	−0.15	−0.63 (✓)	8	2.24
	Oat	0.69	77	−0.03	0.62 (✓)	13	2.45	0.81	67	−0.2	0.31	9	2.88
	Corn	0.44	80	−0.21	−0.05	5	–	–	–	–	–	1	–
	Black Bean	–	–	–	–	1	–	–	–	–	–	1	–
	Alfalfa	–	–	–	–	0	–	–	–	–	–	0	–
	Overall	0.48	58	−0.08	0.56 (✓)	93	2.55	0.61	71	−0.08	0.64 (✓)	44	4.5

located in the Canadian Prairies. The reference dataset covered the period from leaf emergence to approximately peak biomass with the exception of corn, suggesting it is useful for assessing the SL2P algorithm at both low and high vegetation density although the validation is not representative of the ability of SL2P to monitor the entire growth cycle of the crops considered. The total of 720 in-situ measurements for LAI, 720 in-situ measurements fCover, and 360 for CWC offer sufficient sampling to provide validation statistics representative of typical ranges of variables although the sampling was not sufficiently regular to represent APU statistics as a function of the magnitude of a given variable. This led to our use of the slope to assess the trends in bias with the magnitude of a variable and the UAR statistic to represent uncertainty in a manner invariant of the magnitude of a variable.

The in-situ dataset spanned 150 ESUs for seven crop types (soybeans, wheat, canola, oat, corn, black-bean and alfalfa). Due to limited sampling comparisons, comparison metrics over only black-bean or alfalfa were not considered sufficiently precise for further discussion; they have been used only to compute statistics over all crop-types combined. Since most crops were sampled within typically the same image swath, the dataset provided a useful comparison of algorithm performance as crop type varied but the sensitivity of algorithms performance to factors related to using only one geographic location (acquisition geometry, phenology, soils, topography and cropping practices and the continental atmospheric conditions) was not quantified. Moreover, due to differences between MSI and OLI cloud-free acquisition dates, the dataset was not considered suitable for an unbiased comparison of the performance of MSI/SL2P versus OLI/SL2P based estimates using the SL2P algorithm.

Considering punctual comparisons, LAI and CWC were underestimated by MSI/SL2P (slope (bias) = 0.70 (−0.37) for LAI and 0.42 (−0.37 kg/m^2) for CWC) and OLI/SL2P (slope (bias) = 0.59 (−1.21) for LAI and 0.24 (−0.23 kg/m^2) for CWC). In contrast, fCover estimates from SL2P were relatively unbiased for both sensors (slope (bias) = 0.99 (1.84%) using MSI/SL2P and 0.93 (−3.75%) using OLI/SL2P). In terms of uncertainty, the RMSE for MSI/SL2P (OLI/SL2P) estimates was 0.98 (1.63) for LAI, 11.39% (10.95%) for fCover and 0.66 kg/m^2 (0.69 kg/m^2) for CWC for MSI/SL2P. 84% (87%) of fCover estimates using MSI/SL2P (OLI/SL2P) meets SEN4SCI uncertainty requirements, in comparison to 80% (44%) for LAI estimates, and 33% (45%) for CWC. The SL2P processor also provides theoretical error estimates (Weiss et al., 2016). Overall RMSE values obtained for LAI are found close to the processor theoretical performances (RMSE = 0.89). However, for fCover (CWC), the RMSE is found to be ~3 times (~2 times) greater than the theoretical value (4% (0.3 kg/m^2)) although these theoretical error estimates are optimistic as they are based on simulations using a homogenous canopy radiative transfer model. Using simulated MSI data and RT-ANN combination, Camacho et al. (2013b) reported RMSE = 1.4 (0.29 kg/m^2), bias = −0.46 (0.05 kg/m^2) and slope = 1.32 (0.28) between LAI (CWC) estimates and in-situ data over agricultural sites located in Barrax. Richter et al. (2009) and Delegido et al. (2013) found that MSI bands exhibited greater sensitivity to variations in biophysical variables in comparison to similar OLI bands leading them to suggest that the potential uncertainty in MSI based estimation algorithms should be lower than equivalent algorithms applied to OLI measurements. Moreover, Richter et al. (2012) showed that NIR and red-edge spectral regions provide the most relevant information to estimate LAI from MSI data using RT-ANN combination; and that the best result is an RMSE equal to 0.53 in comparison to in-situ measurements acquired over agricultural sites located in Barrax (Spain). Fang et al. (2003) showed that a surface reflectance error of 1% causes about 0.04 error for LAI estimates using a RT-ANN combination. Similarly, Djamai and Fernandes (2018) showed that, for flat areas, a 1% of surface reflectance error could generate 0.09 error for LAI, 1% error for fCover and lower than 0.01 kg/m^2 error for CWC using the SL2P processor. These results suggest that the higher error in CWC estimates are mainly caused by the SL2P processor itself rather than radiometric calibration errors.

SL2P processor performances depended strongly on the crop type and the biophysical variable. SL2P LAI estimates performed better for soybean and canola in comparison to their performances for other crop types; notably for corn for which a substantial overestimation was observed. These may be due to the turbid medium assumption (Combal et al., 2003) of the SAILH model used to train SL2P that contrasts with the relatively clumped row structure of corn crops. For CWC, soybean

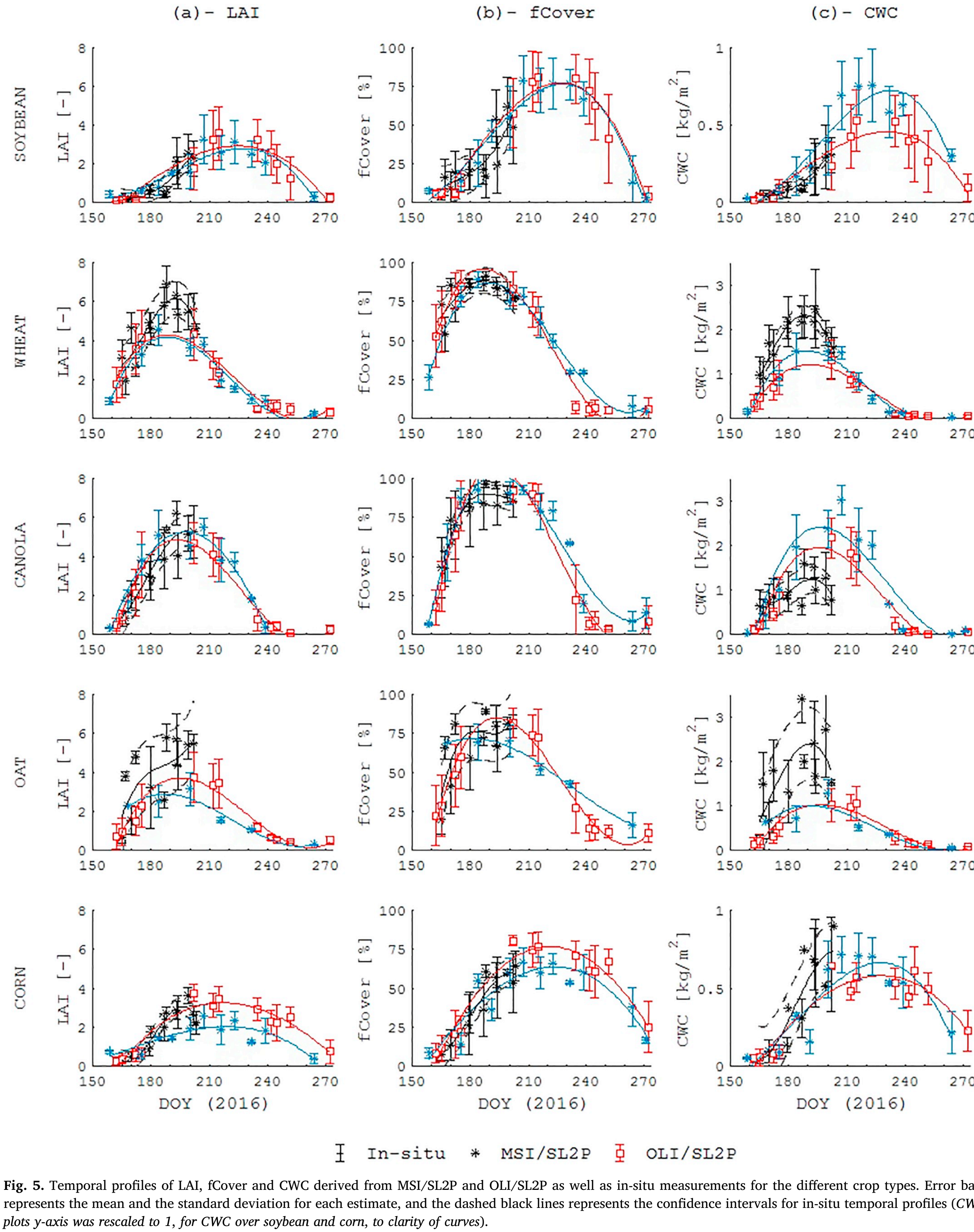

Fig. 5. Temporal profiles of LAI, fCover and CWC derived from MSI/SL2P and OLI/SL2P as well as in-situ measurements for the different crop types. Error bars represents the mean and the standard deviation for each estimate, and the dashed black lines represents the confidence intervals for in-situ temporal profiles (*CWC plots y-axis was rescaled to 1, for CWC over soybean and corn, to clarity of curves*).

Table 11
Intercomparison statistics between LAI, fCover and CWC time series derived from in-situ measurements, MSI/SL2P and OLI/SL2P.

Biophysical variable	Crop type	ESU number (min – max)	In-situ - MSI/SL2P			In-situ - OLI/SL2P			MSI/SL2P - OLI/SL2P		
			R^2	RMSE	Bias	R^2	RMSE	Bias	R^2	RMSE	Bias
LAI [−]	Soybean	9–27	0.99	0.43	−0.2	0.80	0.41	−0.03	0.95	0.28	−0.22
	Wheat	3–27	0.85	0.44	−0.29	0.53	1.30	−1.22	0.99	0.20	−0.18
	Canola	6–24	0.86	0.65	0.25	0.71	1.00	0.57	0.96	0.50	0.42
	Oat	3–9	–	–	–	–	–	–	0.88	0.68	−0.51
	Corn	3–12	0.99	0.56	0.32	0.85	0.88	−0.74	0.83	0.99	−0.89
fCover [%]	Soybean	9–27	0.99	4.26	−3.27	0.88	7.56	4.78	0.99	2.39	−1.28
	Wheat	3–27	0.98	4.81	3.01	0.98	3.28	−1.91	0.97	8.64	−1.00
	Canola	6–24	0.98	6.90	−1.41	0.95	5.67	3.57	0.99	8.82	4.51
	Oat	3 - 9	–	–	–	–	–	–	0.89	12.63	0.77
	Corn	3 - 12	0.98	10.99	7.34	0.60	11.56	−2.20	0.99	10.11	−8.89
CWC [kg/m^2]	Soybean	1–9	0.91	0.05	−0.02	0.99	0.07	0.06	0.99	0.17	0.14
	Wheat	3–27	0.51	0.67	−0.62	0.32	0.69	−0.65	0.98	0.20	0.14
	Canola	2 - 8	0.95	0.68	0.35	0.91	0.81	0.57	0.99	0.41	0.41
	Oat	3 - 9	–	–	–	–	–	–	0.91	0.11	−0.04
	Corn	1 - 5	0.98	0.06	−0.05	0.57	0.08	−0.07	0.94	0.06	0.02

and corn generally resulted in better agreement statistics between SL2P estimates and in-situ measurements. We hypothesize that the large underestimation of CWC for wheat and oat observed using SL2P with either sensor was due to two factors: i) the inclusion of stems within in-situ measurements for these crops as the SL2P estimates consider only foliage and ii) the typical underestimation of LAI by SL2P for the different crop types as CWC was computed as LAI x C_w. The low agreement for SL2P estimates over canola during the crop flowering stage (DOY from 180 to 203) may also be due to absence of flowers within the PROSAILH simulations used when calibrating SL2P.

Using locally calibrated VI models, better agreement statistics are generally obtained in comparison to agreement statistics when comparing SL2P estimates to the same measurements. For example, the RMSE between in-situ data and MSI/VI (OLI/VI) estimates was 0.69 (0.95) for LAI, 12.52% (9.48%) for fCover and 0.48 kg/m^2 (0.61 kg/m^2) for CWC. However, locally calibrated CWC estimates derived from MSI and OLI data saturates for moderate to high values, confirming previous findings (Chen et al., 2005; Jackson et al., 2004), in contrast to CWC estimates derived from MSI/SL2P and OLI/SL2P.

Prior comparison between RT-ANN combination and locally calibrated VI models to estimate LAI over agricultural sites was conducted by Walthall et al. (2004). They showed that VI models (RMSE = 0.44; R^2 = 0.87) outperform RT-ANN (RMSE = 0.63; R^2 = 0.63). Both their work and our results indicate that there is room for reduction in LAI bias through locally calibrated algorithms but less so for fCover. The precision of CWC estimates was insufficient to determine if bias removal would reduce uncertainty. Weiss et al. (2007) showed that LAI estimates derived from SPOT-VEGETATION data using RT-ANN combination (RMSE = 0.73) outperforms MODIS collection 4 (RMSE = 1.29) and ECOCLIMAP (Masson et al., 2003; RMSE = 2.15) products over the BELMANIP representative set of sites.

With regards to interpolated time series, we hypothesized that the increased temporal sampling density of in-situ data would result in comparable residuals and bias in comparison to punctual comparisons only. LAI and fCover time series from both MSI/SL2P and OLI/SL2P showed high determination coefficients ($R^2 \geq 0.53$) and low RMSE (bias) (≤1.30 (1.22) for LAI; ≤11.56% (7.34%) for fCover) in comparison to interpolated in-situ data time series. Camacho et al. (2013b) reported comparable determination coefficient (R^2 = 0.55) over Barrax agricultural sites. For CWC, time series confirmed the previously noted substantial underestimation of SL2P estimates over wheat (≈0.67 kg/m^2 (−0.62 kg/m^2)) irrespective to the sensor. Although time series for oat are not analysed in Section 4.2 due to their large confidence intervals, Fig. 5 indicates substantial underestimation of CWC estimates for oat as well. The uncertainty results obtained from interpolated time series were generally, but not always, comparable to statistics obtained for cross-validation: 58% (90%) of times the difference between RMSE values was found lower than 10% (20%) of in-situ data average value. An exception was an overestimation of temporal CWC estimates for canola (RMSE (bias) ≥ 0.68 kg/m^2 (≥0.35 kg/m^2) irrespective to the sensor) that was not indicated during the cross-validation. This highlights the importance of using both cross-validation errors and comparisons using interpolated time series as a good practice for validating decametric resolution remote sensing products sparsely sampled in time. Except for wheat (R^2 = 0.51 using MSI/SL2P and R^2 = 0.32 using OLI/SL2P) and corn using OLI/SL2P (R^2 = 0.57), determination coefficients between estimates and interpolated in-situ CWC time series ($R^2 \geq 0.91$) were found higher than the determination coefficient reported by Camacho et al. (2013b) over Barrax agricultural sites (R^2 = 0.59), determination coefficients ($R^2 \geq 0.70$) between CWC retrievals from MODIS data calibrated using PROSAILH simulations and in-situ data acquired over study sites of chaparral vegetation in California (Zarco-Tejada et al., 2003); and determination coefficient (R^2 = 0.71) between CWC retrievals from MODIS data using PROSAILH-ANN combination and AVIRIS estimates (Cheng et al., 2006) over four different ecosystems in United-States (Trombetti et al., 2008).

MSI/SL2P and OLI/SL2P time series also showed low error (RMSE (bias) ≤ 0.99 (0.89) for LAI, ≤12.63% (8.89%) for fCover and ≤0.32 kg/m^2 (0.31 kg/m^2) for CWC) and high R^2 (≥0.83 irrespective of the biophysical variable) amongst themselves, suggesting the possibility of blending the products to improve the temporal monitoring of biophysical variables at decametric scale.

The study presented here validated estimates of three biophysical variables from the SL2P processor using TOC reflectance data from two different sensors, and compared these estimates to a locally calibrated empirical model. However, the study had limitations including i) the contrast between datasets used to validate estimates from MSI/SL2P and estimates from OLI/SL2P ii) the irregular sample size by crop type and by biophysical variable iii) missing the maximum growth stage of corn and the period past-peak growth for all crops iv) the limited spatial and temporal extends of our study leading to a limited sampling of atmospheric conditions and illumination geometry, iv) the lack of additional globally applicable algorithms to further understand the sensitivity to both errors in input reflectance and prior assumptions regarding surface conditions.

6. Conclusion

The objective of this study is to validate three vegetation biophysical variables (LAI, fCover and CWC) derived from Sentinel-2/MSI and Landsat-8/OLI data using the SL2P processor over an agricultural site located in the Canadian Prairies. This objective is achieved, with the exception of CWC where more samples are needed. Results showed that, although the uncertainty requirements from SEN4SCI are not entirely satisfied, SL2P presents good performances to estimate LAI and fCover from both MSI and OLI data; low biases were generally obtained for both. However, CWC estimates were worse than expected; more work is required to understand why the algorithms performed lower for this variable. Temporal interpolation works well for increasing matches between in-situ and image products, with a minor reduction in precision compared to increasing the spatial sampling over larger regions. Both MSI and SL2P sampling is sufficient for reconstructing profiles but more research is required with more extensive sampling. Based on the results from this experiment, we recommend to (1) report UAR statistics for future validation studies as a measure of to what extent products meet the mission requirements, (2) evaluate the potential to reduce bias on SL2P estimates by crop specific calibrations (3) evaluate the potential for improving the time sampling and estimation accuracy by combining OLI and MSI data.

Acknowledgments

The authors wish to acknowledge the Canadian Space Agency and Natural Resources Canada for supporting this work, the European Space Agency and the United States Geological Survey for provision of datasets. The authors also thank all of the participants in The SMAP Validation Experiment 2016 and their funding agencies.

References

Abuelgasim, A., Fernandes, R., Leblanc, S., 2006. Evaluation of national and global LAI products derived from optical remote sensing instruments over Canada. IEEE Trans. Geosci. Remote Sens. 44, 1872–1884.
ANSI/ASME, 1985. Supplement to ASME Performance Test Codes 19.1-1985. Instruments and Apparatus. Part 1-Measurement Uncertainty The American Society of Mechanical Engineers, New York.
Asrar, G., 1989. Theory and Applications of Optical Remote Sensing. Wiley, New York, pp. 142–335.
Asrar, G., Kanemasu, E.T., Yoshida, M., 1985. Estimates of leaf area index from spectral reflectance of wheat under different cultural practices and solar angle. Remote Sens. Environ. 17, 1–11.
Bacour, C., Baret, F., Beal, D., Weiss, M., Pavageau, K., 2006. Neural network estimation of LAI, fAPAR, fCover and LAIxCab, from top of canopy MERIS reflectance data: principles and validation. Remote Sens. Environ. 105, 313–325.
Baret, F., Buis, S., 2008. Estimating canopy characteristics from remote sensing observations: Review of methods and associated problems. In: Liang, S. (Ed.), Advances in Land Remote Sensing: System. Modeling, Inversion and Application, pp. 171–200.
Baret, F., Guyot, G., 1991. Potentials and limits of vegetation indices for LAI and APAR assessment. Remote Sens. Environ. 35, 161–173.
Baret, F., Morissette, J., Fernandes, R., Champeaux, J.L., Myneni, R., Chen, J., Plummer, S., Weiss, M., Bacour, C., Garrigues, S., Nickeson, J.E., 2006. Evaluation of the representativeness of networks of sites for the validation and inter-comparison of land biophysical products. Proposition of the CEOS-BELMANIP. IEEE Trans. Geosci. Remote Sens. 44, 1794–1803.
Baret, F., Hagolle, O., Geiger, B., Bicheron, P., Miras, B., Huc, M., Berthelot, B., Niño, F., Weiss, M., Samain, O., Roujean, J.L., Leroy, M., 2007. LAI, fAPAR and fCover CYCLOPES global products derived from VEGETATION: part 1: principles of the algorithm. Remote Sens. Environ. 110, 275–286.
Baret, F., Weiss, M., Lacaze, R., Camacho, F., Makhmara, H., Pacholczyk, P., Smets, B., 2013. GEOV1: LAI and FAPAR essential climate variables and FCOVER global time series capitalizing over existing products. Part1: principles of development and production. Remote Sens. Environ. 137, 299–309.
Best, R.G., Harlan, J.C., 1985. Spectral estimation of green leaf area index of oats. Remote Sens. Environ. 17, 27–36.
Bhuiyan, H.A.K.M., McNairn, H., Powers, J., Friesen, M., Pacheco, A., Jackson, T.J., Cosh, M.H., Colliander, A., Berg, A., Rowlandson, T., Bullock, P., Magagi, R., 2018. Assessing SMAP soil moisture scaling and retrieval in the Carman (Canada) study site. Vadose Zone J. 17, 180132. https://doi.org/10.2136/vzj2018.07.0132.
Bunnik, N.J.J., 1978. The Multispectral Reflectance of Shortwave Radiation by Agricultural Crops in Relation with their Morphological and Optical Properties. Mededelingen Landbouwhogeschool, Wageningen, The Netherlands (172 pp).
Camacho, F., Cernicharo, J., Lacaze, R., Baret, F., Weiss, M., 2013a. GEOV1: LAI, FAPAR essential climate variables and FCOVER global time series capitalizing over existing products. Part 2: validation and intercomparison with reference products. Remote Sens. Environ. 137, 310–329.
Camacho, F., Baret, F., Weiss, M., Fernandes, R., Berthelot, B., Sánchez, J., Latorre, C., García-Haro, J., Duca, R., 2013b. Validación de algoritmos para la obtención de variables biofísicas con datos Sentinel2 en la ESA: proyecto VALSE-2. XV Congreso de la Asociación Española de Teledetección, INTA, Torrejón de Ardoz, Spain. https://doi.org/10.13140/RG.2.1.4655.0241.
Canisius, F., Fernandes, R., 2012. Evaluation of the information content of Medium Resolution Imaging Spectrometer (MERIS) data for regional leaf area index assessment. Remote Sens. Environ. 119, 301–314.
Ceccato, P., Flasse, S., Gregoire, J., 2002. Designing a spectral index to estimate vegetation water content from remote sensing data: part 2. Validation and applications. Remote Sens. Environ. 82, 198–207.
CEOS, 2016. CEOS WGCV terms of reference. Working group on calibration and validation. Version 1.0 / November 2nd, 2016. Available online on. http://ceos.org/document_management/Publications/Governing_Docs/WGCV_ToR-v1.0_02Nov2016.pdf.
Chance, J.E., 1981. Crop identification and leaf area index calculation with Landsat multispectral data. Int. J. Remote Sens. 2, 1–14.
Chen, J.M., 1996. Evaluation of vegetation indices and modified simple ratio for Boreal applications. Can. J. Remote. Sens. 22, 229–242.
Chen, J.M., 2018. Remote sensing of leaf area index and clumping index. In: Liang, Shunlin (Ed.), Chapter in Comprehensive Remote Sensing. vol. 3. Elsevier, Oxford, 9780128032213, pp. 53–77. https://doi.org/10.1016/B978-0-12-409548-9.10540-8.
Chen, D.Y., Huang, J.F., Jackson, T.J., 2005. Vegetation water content estimation for corn and soybeans using spectral indices derived from MODIS near- and short-wave infrared bands. Remote Sens. Environ. 98, 225–236.
Cheng, Y.B., Zarco-Tejada, P.J., Riano, D., Rueda, C.A., Ustin, S.L., 2006. Estimating vegetation water content with hyperspectral data for different canopy scenarios: relationships between AVIRIS and MODIS indexes. Remote Sens. Environ. 105, 354–366.
Claverie, M., Vermote, E.F., Weiss, M., Baret, F., Hagolle, O., Demarez, V., 2013. Validation of coarse spatial resolution LAI and FAPAR time series over cropland in southwest France. Remote Sens. Environ. 139, 216–230.
Combal, B., Baret, F., Weiss, M., Pragnère, A., Trubuil, A., Macé, D., Myneni, R., Knyazikhin, Y., Wang, L., 2003. Retrieval of canopy biophysical variables from bidirectional reflectance using prior information to solve the ill-posed inverse problem. Remote Sens. Environ. 84, 1–15.
Croft, H., Chen, J.M., 2018. Remote sensing of leaf pigments. In: Liang, Shunlin (Ed.), Chapter in Comprehensive Remote Sensing. Elsevier, Oxford, 9780128032213, pp. 117–142. https://doi.org/10.1016/B978-0-12-409548-9.10547-0.
Delegido, J., Verrelst, J., Meza, C., Rivera, J., Alonso, L., Moreno, J., 2013. A red-edge spectral index for remote sensing estimation of green LAI over agroecosystems. Eur. J. Agron. 46, 42–52.
Delloye, C., Weiss, M., Defourny, P., 2018. Retrieval of the canopy chlorophyll content from Sentinel-2 spectral bands to estimate nitrogen uptake in intensive winter wheat cropping systems. Remote Sens. Environ. 216, 245–261.
Deng, F., Chen, J.M., Chen, M., Pisek, J., 2006. Algorithm for global leaf area index retrieval using satellite imagery. IEEE Trans. Geosci. Remote Sens. 44, 2219–2229.
Disney, M., Muller, J.P., Kharbouche, S., Kaminski, T., Voßbeck, M., Lewis, P., Pinty, B., 2016. A new global fAPAR and LAI dataset derived from optimal albedo estimates: comparison with MODIS products. Remote Sens. 8, 275.
Djamai, N., Fernandes, R., 2018. Comparison of SNAP-derived sentinel-2A L2A product to ESA product over Europe. Remote Sens. 10, 926.
Doxani, G., Vermote, E., Roger, J.C., Gascon, F., Adriaensen, S., Frantz, D., Hagolle, O., Hollstein, A., Kirches, G., Li, F., Louis, J., Mangin, A., Pahlevan, N., Pflug, B., Vanhellemont, Q., 2018. Atmospheric correction inter-comparison exercise. Remote Sens. 2018 (10), 352.
Drusch, M., Del Bello, U., Carlier, S., Colin, O., Fernandez, V., Gascon, F., Hoersch, B., Isola, C., Laberinti, P., Martimort, P., Meygret, A., Spoto, F., Sy, O., Marchese, F., Bargellini, P., 2012. Sentinel-2: ESA's optical high-resolution Mission for GMES operational services. Remote Sens. Environ. 20, 25–36.
European Space Agency, 2012. Sentinel-2: ESA's Optical High-Resolution Mission for GMES Operational Services. ESA Communications978-92-9221-419-7.
Fang, H., Liang, S., Kuusk, A., 2003. Retrieving leaf area index using a genetic algorithm with a canopy radiative transfer model. Remote Sens. Environ. 85, 257–270.
Fernandes, R., 2012. Canada Centre for Remote Sensing Protocol for In-situ Leaf Area Index Using Digital Hemispherical Photography Using the INRA CANEYE Analysis System (CCRS Technical Report Series). ftp://ftp.ccrs.nrcan.gc.ca/EMS/LAI/CCRSCaneye.pdf.
Fernandes, R., Leblanc, S.G., 2005. Parametric (modified least squares) and non-parametric (Theil–Sen) linear regressions for predicting biophysical parameters in the presence of measurement errors. Remote Sens. Environ. 95, 303–316.
Fernandes, R., Plummer, S., Nightingale, J., 2014. Global Leaf Area Index Product Validation Good Practices. Committee of Earth Observing Systems Working Group on Calibration and Validation, pp. 75.
Ganguly, S., Nemani, R.R., Zhang, G., Hashimoto, H., Milesi, C., Michaelis, A., Wang, W., Votava, P., Samanta, A., Melton, F., Dungan, J.L., Vermote, E., Gao, F., Knyazikhin, Y., Myneni, R., 2012. Generating global leaf area index from Landsat: algorithm formulation and demonstration. Remote Sens. Environ. 122, 185–202.
Gao, B.C., 1996. NDWI - a normalized difference water index for remote sensing of vegetation liquid water from space. Remote Sens. Environ. 58, 257–266.
Garcia-Haro, F.J., Campos-Taberner, M., Munoz-Mari, J., Laparra, V., Camacho, F., Sanchez-Zapero, J., Camps-Valls, G., 2018. Derivation of global vegetation biophysical parameters from EUMETSAT polar system. ISPRS J. Photogramm. Remote Sens. 139, 57–74.
Garrigues, S., Lacaze, R., Baret, F., Morisette, J.T., Weiss, M., Nickeson, J.E., Fernandes, R., Plummer, S., Shabanov, N.V., Myneni, R.B., Knyazikhin, Y., Yang, W., 2008. Validation and intercomparison of global leaf area index products derived from remote sensing data. J. Geophys. Res. 113, G02028.
Global Climate Observing System, 2016. The global observing system for climate: Implementation needs. In: GCOS Steering Committee at their 24th Meeting in

Guayaquil, Ecuador, in October 2016, Available online on. https://unfccc.int/sites/default/files/gcos_ip_10oct2016.pdf.
Goel, N.S., Deering, D.W., 1985. Evaluation of a canopy reflectance model for LAI estimation through its inversion. IEEE Trans. Geosci. Remote Sens. 23, 674–684.
Group on Earth Observations, 2018. Global agricultural monitoring initiative. Stocktaking overview of the G20. http://www.earthobservations.org/documents/publications/201803_geoglam _g20.pdf.
Irons, J.R., Dwyer, J.L., Barsi, J.A., 2012. The next Landsat satellite: the Landsat data continuity Mission. Remote Sens. Environ. 122, 11–21.
Jackson, J.T., Chen, D., Cosh, M., Li, F., Anderson, M., Walthall, C., Doriaswamy, P., Hunt, E.R., 2004. Vegetation water content mapping using Landsat data derived normalized difference water index for corn and soybeans. Remote Sens. Environ. 92, 475–482.
Jacquemoud, S., Baret, F., 1990. PROSPECT: a model of leaf optical properties spectra. Remote Sens. Environ. 34, 75–91.
Jacquemoud, S., Baret, F., Andrieu, B., Danson, F.M., Jaggard, K., 1995. Extraction of vegetation biophysical parameters by inversion of the PROSPECT + SAIL models on sugar beet canopy reflectance data. Application to TM and AVIRIS sensors. Remote Sens. Environ. 52, 163–172.
Kanemasu, E.T., Niblett, C.L., Manges, H., Lenhert, D., Newman, M.A., 1974. Wheat: its growth and disease severity as deduced from ERTS-1. Remote Sens. Environ. 3, 43–47.
Kimes, D.S., 1981. Remote sensing of temperature profiles in vegetation canopies using multiple view angles and inversion techniques. IEEE Trans. Geosci. Remote Sens. 19, 85–90.
Knight, E.J., Kvaran, G., 2014. Landsat-8 operational land imager design, characterization and performance. Remote Sens. 6, 10286–10305.
Knyazikhin, Y., Martonchik, J.V., Myneni, R.B., Diner, D.J., Running, S.W., 1998. Synergistic algorithm for estimating vegetation canopy leaf area index and fraction of absorbed photosynthetically active radiation from MODIS and MISR data. J. Geophys. Res. 103, 32257–32275.
Liang, S., Li, X., Wang, J., 2012. Advanced Remote Sensing. Terrestrial Information Extraction and Applications. Academic Press is an imprint of Elsevier978-0-12-385954-9.
Liu, H.Q., Huete, A.R., 1995. A feedback based modification of the NDV I to minimize canopy background and atmospheric noise. IEEE Trans. Geosci. Remote Sens. 33, 457–465.
Loboda, T., Krankina, O., Savin, I., Kurbanov, E., Hall, J., 2017. Land management and the impact of the 2010 extreme drought event on the agricultural and ecological Systems of European Russia. In: Gutman, G., Radeloff, V. (Eds.), Land-Cover and Land-Use Changes in Eastern Europe after the Collapse of the Soviet Union in 1991. Springer, Cham.
Malenovsky, Z., Rott, H., Cihlar, J., Schaepman, M.E., Garcia-Santos, G., Fernandes, R., Berger, M., 2012. Sentinels for science: potential of Sentinel-1, -2, and -3 missions for scientific observations of ocean, cryosphere. Remote Sens. Environ. 120, 91–101.
Markham, B., Barsi, J., Kvaran, G., Ong, L., Kaita, E., Biggar, S., Czapla-Myers, J., Mishra, N., Helder, D., 2014. Landsat-8 operational land imager radiometric calibration and stability. Remote Sens. 6, 12275–12308.
Masson, V., Champeaux, J.-L., Chauvin, F., Meriguet, C., Lacaze, R., 2003. A global database of land surface parameters at 1-km resolution in meteorological and climate models. J. Climate 16, 1261–1282.
McNairn, H., Jackson, T.J., Powers, J., Bélair, S., Berg, A., Bullock, P., Colliander, A., Cosh, M.H., Kim, S.B., Magagi, R., Pacheco, A., Merzouki, A., Hosseini, M., Hanis-Gervais, K., 2017. SMAPVEX16 Database Report. pp. 71. Available online. http://smapvex16-mb.espaceweb.usherbrooke.ca/documents/SMAPVEX16-MB_Experimental_Plan.pdf.
Morfitt, R., Barsi, J., Levy, R., Markham, B., Micijevic, E., Ong, L., Scaramuzza, P., Vanderwerff, K., 2015. Landsat-8 operational land imager (OLI) radiometric performance on-orbit. Remote Sens. 7, 2208–2237.
Morisette, J., Baret, F., Liang, S., 2006. Special issue on global land product validation. IEEE Trans. Geosci. Remote Sens. 44, 1695–1697.
Mueller-Wilm, U., Devignot, O., Pessiot, L., 2017. Sen2Cor configuration and user manual. S2-PDGS-MPC-L2A-SUM-V2.4. Issue 1. Available online. http://step.esa.int/thirdparties/sen2cor/2.4.0/Sen2Cor_240_Documenation_PDF/S2-PDGS-MPC-L2A-SUM-V2.4.0.pdf.
Pearson, R.L., Miller, L.D., 1972. Remote mapping of standing crop biomass for estimation of the productivity of the shortgrass prairie. In: Proceedings of the Eighth International Symposium on Remote Sensing of Environment. Environmental Research Institute of Michigan, Ann Arbor, MI, pp. 1357–1381.
Pisek, J., Chen, J.M., 2007. Comparison and validation of MODIS and VEGETATION global LAI products over four BigFoot sites in North America. Remote Sens. Environ. 109, 81–94.
Pollock, R.B., Kanemasu, E.T., 1979. Estimating leaf-area index of wheat with LANDSAT data, Remote Sens. Environ. 8, 307–312.
Richter, K., Atzberger, C., Vuolo, F., Weihs, P., D'Urso, G., 2009. Experimental assessment of the sentinel-2 band setting for RTM-based LAI retrieval of sugar beet and maize. Can. J. Remote. Sens. 35, 230–247.
Richter, K., Hank, T.B., Vuolo, F., Mauser, W., D'Urso, G., 2012. Optimal exploitation of the Sentinel-2 spectral capabilities for crop leaf area index mapping. Remote Sens. 4, 561–582.
Ross, J., 1975. Radiative transfer in plant communities. In: Monteith, J.L. (Ed.), Vegetation and the Atmosphere. Academic Press, London, pp. 13 ± 55.
Rouse, J.W., Haas, R.H., Schell, J.A., Deering, D.W., 1974. Monitoring vegetation system in the great plains with ERTS. In: Proceedings of the Third Earth Resources Technology Satellite-1 Symposium, Greenbelt, USA, NASASP-351, pp. 3010–3017.
Snee, R., 1977. Validation of regression models: methods and examples. Technometrics 19, 415–428.
Suits, G.H., 1972. The calculation of the directional reflectance of a vegetative canopy. Remote Sens. Environ. 2, 117–125.
Teillet, P.M., Staenz, K., William, D.J., 1997. Effects of spectral, spatial, and radiometric characteristics on remote sensing vegetation indices of forested regions. Remote Sens. Environ. 61, 139–149.
Trombetti, M., Riaño, D., Rubio, M.A., Cheng, Y.B., Ustin, S.L., 2008. Multi-temporal vegetation canopy water content retrieval and interpretation using artificial neural networks for the continental USA. Remote Sens. Environ. 112, 203–215.
Verhoef, W., 1984. Light scattering by leaf layers with application to canopy reflectance modeling: the SAIL model. Remote Sens. Environ. 16, 125–141.
Verrelst, J., Rivera, J.P., Veroustraete, F., Muñoz-Marí, J., Clevers, J.G.P.W., Camps-Valls, G., Moreno, J., 2015. Experimental Sentinel-2 LAI estimation using parametric, non-parametric and physical retrieval methods – a comparison. ISPRS J. Photogramm. Remote Sens. 108, 260–272.
Walthall, C., Dulaney, W., Anderson, M., Norman, J., Fang, H., Liang, S., 2004. A comparison of empirical and neural network approaches for estimating corn and soybean leaf area index from Landsat ETM+ imagery. Remote Sens. Environ. 92, 465–474.
Weigand, C.L., Richardson, A.J., Kanemasu, E.T., 1979. Leaf area index estimates for wheat from LANDSAT and their implications for evapotranspiration and crop modeling. Agron. J. 71, 336–342.
Weiser, R.L., Asrar, G., Miller, G.P., Kanemasu, E.T., 1986. Assessing grassland characteristics from spectral measurements. Remote Sens. Environ. 20, 141–152.
Weiss, M., Baret, F., 1999. Evaluation of canopy biophysical variable retrieval performances from the accumulation of large swath satellite data. Remote Sens. Environ. 70, 293–306.
Weiss, M., Baret, F., 2016. S2ToolBox level 2 products. Version 1.1. Available online. step.esa.int/docs/extra/ATBD_S2ToolBox_L2B_V1.1.pdf.
Weiss, M., de Beaufort, L., Baret, F., Allard, D., Bruguier, N., Marloie, O., 2001. Mapping leaf area index measurements at different scales for the validation of large swat satellite sensors: First results of the VALERI project. In: Physical Measurements and Signatures in Remote Sensing. Guyot and Phulpin, pp. 125–130.
Weiss, M., Baret, F., Garrigues, S., Lacaze, R., 2007. LAI and fAPAR CYCLOPES global products derived from VEGETATION. Part 2: validation and comparison with MODIS collection 4 products. Remote Sens. Environ. 110, 317–331.
Zarco-Tejada, P.J., Rueda, C.A., Ustin, S.L., 2003. Water content estimation in vegetation with MODIS reflectance data and model inversion methods. Remote Sens. Environ. 85, 109–124.

Web references

CanEye, 2018. accessed in June. https://www6.paca.inra.fr/can-eye/.
The SMAP validation experiment 2016 in Manitoba (SMAPVEX16-MB, accessed in June 2018). http://smapvex16-mb.espaceweb.usherbrooke.ca/home.php.
The Committee of Earth Observing Systems Land Product Validation, 2019The Committee of Earth Observing Systems Land Product Valid. CEOS LPV. accessed in January. https://lpvs.gsfc.nasa.gov/.
The Government of Canada GeoGratis platform, 2018. accessed in June. http://geogratis.cgdi.gc.ca/.
The Integrated Carbon Observation System, 2019. ICOS, accessed in January. http://european-webcam-network.net/.
The Joint Experiment for Crop Assessment and Monitoring, 2019. JECAM. accessed in January. http://www.jecam.org/.
The Landsat Science Team https://landsat.usgs.gov/landsat-science-teams, Accessed date: October 2018.
The Landsat Surface Reflectance Code, 2018. LaSRC, accessed in October. https://landsat.usgs.gov/sites/default/files/documents/lasrc_product_guide.pdf.
The National Ecological Observatory Network NEON. https://www.neonscience.org/, Accessed date: January 2019.
The Sentinel Application Platform http://step.esa.int/main/toolboxes/snap/, Accessed date: June 2018.
The Sentinels for Science (SEN4SCI) expert consultation activity, 2018SCI) expert consultation acti. accessed in October. http://www.geo.uzh.ch/microsite/sen4sci.
The Terrestrial Ecosystem Research Network, 2019. TERN, accessed in January. http://www.phenocam.org.au.